Local Measurement of Nonclassical Ion Heating during Magnetic Reconnection

S. C. Hsu,* G. Fiksel,† T. A. Carter, H. Ji, R. M. Kulsrud, and M. Yamada

Princeton Plasma Physics Laboratory, P.O. Box 451, Princeton, New Jersey 08543

(Received 23 November 1999; revised manuscript received 1 March 2000)

Local ion temperature and flows are measured directly in the well-characterized reconnection layer of a laboratory plasma. The measurements indicate strongly that ions are heated due to reconnection and that more than half of the reconnected field energy is converted to ion thermal energy. Neither classical viscous damping of the observed sub-Alfvénic ion flows nor classical energy exchange with electrons is sufficient to account for the ion heating, suggesting the importance of nonclassical dissipation mechanisms in the reconnection layer.

PACS numbers: 52.20.–j, 52.30.Jb, 96.60.Rd

Magnetic reconnection [1] has been invoked often to explain the acceleration and heating of plasma particles. Solar observations suggest that hard x-rays from solar flares are produced by reconnection [2], and it has been proposed that the million degree corona is heated by turbulent reconnection [3]. In the Earth's magnetosphere, reconnection is believed to occur in the day-side magnetopause and in the magnetotail, where charged particles can be accelerated along field lines toward the polar regions, giving rise to the aurora [4]. In laboratory plasmas such as reversed-field pinches, enhanced ion heating has been seen to correlate with magnetic fluctuations associated with reconnection and dynamo activity [5]. However, in all these environments, it has not yet been possible to measure the complete reconnection magnetic field topology together with the detailed spatial and temporal characteristics of any resultant particle energization. Therefore, a rigorous demonstration of both these aspects simultaneously would have important implications.

Laboratory experiments have made important contributions toward understanding reconnection. In the pioneering UCLA experiments, ion acceleration, possibly modified by wave turbulence [6], and electron heating [7] were observed. However, ion heating could not be addressed because these experiments were in the "electron MHD" regime in which $\rho_i \gg L$. In TS-3 at the University of Tokyo, toroidal Alfvénic flows were believed to be accelerated by the strong tension force of reconnected field lines, and global ion heating was attributed to thermalization of the sheared Alfvénic flows [8]. In SSX (Swarthmore Spheromak Experiment), Alfvénic ion jets correlated with reconnection were reported based on measurements of ion flux at the vacuum wall [9]. In both TS-3 and SSX, reconnection occurs when two spheromaks collide at a substantial fraction of the Alfvén speed. Thus, effects such as strong compressional heating or conversion of the translational energy of the spheromaks could complicate the interpretation of any observed ion acceleration and/or heating. It should also be noted that in TS-3 the ion temperature was inferred from chord averaged neutral and impurity ion emission, and on SSX, the interpretation of Alfvénic ion flow is not unique based on the measurements reported.

In this work, ion heating during reconnection is studied in a controlled and well-characterized reconnection layer. The significant new result is the clear demonstration of enhanced, nonclassical ion heating in a 2D reconnection layer. Downstream ion flows are observed to be energetically insignificant ($V_i \sim 0.25 V_A$), and viscous damping of the flows cannot explain the observed ion heating. Ions also cannot be heated classically by electrons because the energy relaxation time ($\sim$400 μs) is much longer than the reconnection time ($\sim$30 μs); furthermore, the energy released due to classical dissipation is an order of magnitude too small. Based on these results, an ion energy balance is derived, showing that the ion heating must have occurred due to nonclassical processes, e.g., via wave-particle interactions [10] or collisionless inertial effects [11].

Experiments were performed on MRX (Magnetic Reconnection Experiment) [12], which produces plasmas satisfying the MHD criteria globally (Lundquist number $S \gg 1$, $\rho_i \ll L$, $V_A \ll c$). Formation and control of the reconnection layer in MRX is unique among laboratory experiments. "Flux cores" containing toroidal field (TF) and poloidal field (PF) coils allow the controlled formation of a toroidal 2D reconnection layer, shown schematically in Fig. 1. The arrows represent the motion of plasma and magnetic flux during "pull" reconnection, in which public flux linking both flux cores is reconnected into private flux linking each individual flux-core. This sequence produces a reconnection layer elongated in Z which persists for more than ten Alfvén transit times ($\tau_A \approx 2.5$ μs). When the TF coils are connected with opposite (same) polarity, the out-of-plane field B_θ is negligible (finite), resulting in null-helicity (co-helicity) reconnection. Results reported in this paper are from null-helicity experiments. Previously, the detailed structure of the reconnection layer was reported [13], revealing Y-shaped (O-shaped) diffusion regions in the null-helicity (co-helicity) case and a neutral sheet half-thickness $\delta \sim c/\omega_{pi} \sim \rho_i \sim 2$ cm. The reconnection rate was found to be consistent with a generalized Sweet-Parker model [14] in which effects of compressibility, downstream pressure, and nonclassical resistivity are considered.

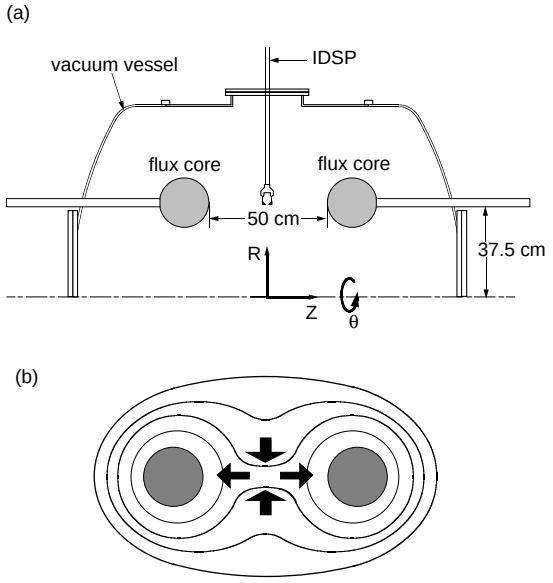

FIG. 1. (a) Schematic of the MRX upper half plane, showing the placement of flux cores and IDSP. (b) Illustration of "pull" reconnection in which "public" poloidal flux reconnects into "private" poloidal flux.

All three components of **B** are measured using magnetic probe arrays, and electron density n_e and temperature T_e are measured using a triple Langmuir probe. Other reconnection quantities are inferred from the direct measurements, including the poloidal flux $\psi \equiv \int_0^R 2\pi R' B_Z(R')\, dR'$ (assuming axisymmetry), current density $j_\theta \approx -(\partial B_Z/\partial R)/\mu_0$, reconnection electric field $E_\theta = -(\partial\psi/\partial t)/2\pi R$, resistivity in the reconnection layer $\eta^* \equiv E_\theta/j_\theta$, perpendicular Spitzer resistivity η_{Sp}, Alfvén speed $V_A \equiv B/\sqrt{\mu_0\rho}$, and plasma inflow speed $V_R \approx -(\partial\psi/\partial t)/(\partial\psi/\partial R)$ (invoking flux freezing outside the diffusion region). The present experiments use pure helium discharges in order to achieve a direct measurement of T_i via Doppler spectroscopy of singly ionized helium. Parameters for the present experiments are as follows: $n_e \approx 5 \times 10^{13}$ cm^{-3} and $T_i \sim T_e \approx 15$ eV in the reconnection layer, $B \approx 250$ G at the edge of the layer, and $S \approx 200$. Qualitative features of the reconnection layer for the present helium discharges are similar to those of previously reported hydrogen discharges, except $\delta_{He} \approx 2\delta_H$, consistent with the previously reported $\delta \sim \rho_i$ scaling [13]. Spatially, the reconnection region is located in an area given by $R \approx 35 \rightarrow 40$ cm and $Z \approx -10 \rightarrow 10$ cm.

A major new accomplishment of this work is the local measurement of T_i using the Ion Dynamics Spectroscopy Probe (IDSP) [15] developed at UW–Madison. The IDSP is an insertable probe which collects plasma light from a localized volume. Two perpendicular lines of sight can give simultaneous Doppler broadening and relative Doppler shift information, although only one line of sight is used for the present experiments. Figure 1(a) shows the placement of the IDSP in MRX (to scale); the lines of sight can be oriented in an R-Z or R-θ plane. Further details of the probe are described elsewhere [15]. Plasma light is delivered via fiber optics to a 1 m monochromator (0.05 Å resolution) and imaged with a gated charge-coupled device (CCD) camera (wavelength resolution of 0.074 Å/pixel). The reported T_i values are determined by fitting He II 4686 Å spectra to a single Gaussian convolved with the known instrumental broadening, an example of which is shown in Fig. 2. The approximately 0.2 Å of fine structure in this emission line (slightly less than instrumental broadening) has been determined to be unimportant. Time resolution is limited by available light, requiring a CCD gate-open time of ≥ 10 μs. Stark broadening is negligible, and IDSP perturbation of the plasma was seen to be minimal after 15 conditioning discharges. IDSP Doppler shifts are used to calibrate Mach probe measurements of ion flow speed derived from an unmagnetized fluid sheath theory [16] generalized for $T_i \approx T_e$.

Two sets of experiments with identical helium fill pressure and discharge voltage demonstrate that an observed rise in T_i is a consequence of reconnection. First, the time evolution of T_i in the center of the reconnection region (IDSP light collected between $R = 35 \rightarrow 40$ cm and $Z = -2.5 \rightarrow 2.5$ cm; denote this area A) is obtained for two situations: with and without reconnection. Pull reconnection is driven by allowing the PF current to ramp down after reaching its peak, which induces the requisite E_θ in the plasma from $t \approx 250 \rightarrow 280$ μs. To omit reconnection, the PF circuit is shorted out near the peak current so that a much smaller E_θ is induced. The T_i rises by more than a factor of 3 when reconnection is driven and much less so when it is not driven, as shown in Fig. 3 (top). Error bars in the ordinate represent 1 standard deviation in an ensemble of T_i measurements (5–10 discharges), and error bars in the abscissa represent the CCD gate time. The initial $T_i \approx 3$–6 eV before $t = 245$ μs, common to both cases, is believed to result from dynamics of plasma formation. The magnetic energy dissipated per unit volume at the center of the current sheet is shown in Fig. 3 (bottom). Note the remarkable correlation between the rise in T_i and the magnetic energy released during reconnection. In the

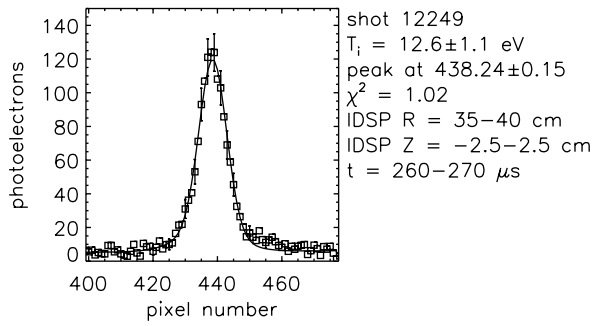

FIG. 2. Doppler broadened profile of He II 4686 Å fitted by the convolution of a Gaussian and instrumental broadening.

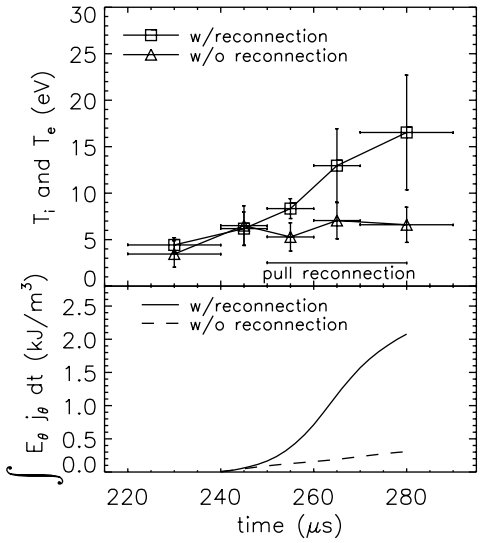

FIG. 3. Time evolution of (top) T_i and (bottom) magnetic energy dissipated per unit volume, both in the center of the reconnection layer, indicating the causality between reconnection and T_i rise.

second set of experiments, the IDSP was scanned in R at two times, $t = 250 \rightarrow 260$ μs and $t = 260 \rightarrow 270$ μs, revealing a localization of the T_i rise in the reconnection layer, as shown in Fig. 4. The measured temporal and spatial characteristics of T_i clearly demonstrate causality between reconnection and the observed rise in T_i.

In classical MHD models of reconnection [1], ions could be heated in the layer through Coulomb interactions with Ohmically heated electrons or downstream from the layer via viscous damping of an Alfvénic outflow. In the present experiments, neither process is sufficient. First, the ion-electron energy relaxation time is several hundred microseconds, much longer than the entire reconnection process, and therefore classical Coulomb interactions between ions and electrons are not relevant. Second, the sheared downstream ion flow speed V_{iZ} during reconnection has been measured by a Mach probe to increase linearly along the layer ($Z = 0 \rightarrow 10$ cm, $R = 38$ cm) from 0 to only 8 km/s ($\approx 0.25 V_A$), as shown in Fig. 5.

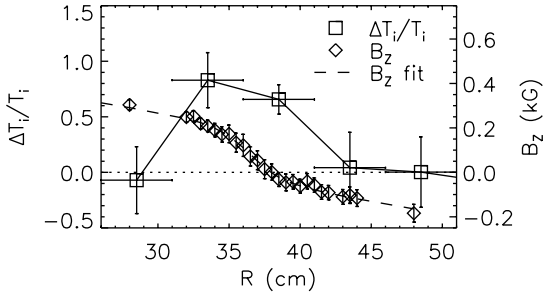

FIG. 4. Radial profiles of the relative rise of T_i from 250–270 μs and reconnecting field B_Z averaged over the same time. Substantial rise in T_i occurs in the reconnection layer (between the knees of the B_Z profile).

The maximum energy density of this flow is an order of magnitude smaller than the observed ion thermal energy density. Furthermore, classical viscous damping of this flow cannot account for the observed ion heating. The sub-Alfvénic V_{iZ} in MRX is consistent with a high downstream pressure [14] which reduces the ∇p force along Z.

An ion energy balance [17] for the reconnection process can be determined. The total magnetic field energy dissipated due to reconnection from $t_1 = 245$ μs $\rightarrow t_2 = 265$ μs in volume V (the area A revolved around the axis of symmetry) is $W_{rec} \equiv \int_V [\int_{t_1}^{t_2} E_\theta(t) j_\theta(t)\, dt]\, d^3V \approx 4.8 \pm 0.7$ J for the discharge conditions pertaining to Figs. 3 and 4. The total ion energy $W_{ions} \approx 3.1 \pm 1.0$ J is the sum of (1) an increase in ion thermal energy $\Delta W_{th,i} \equiv (3/2) \int_V [n(t_2) T_i(t_2) - n(t_1) T_i(t_1)]\, d^3V \approx 0.5 \pm 0.2$ J, (2) directed flow energy $W_{outflow} \equiv \int_V (\rho V_i^2/2)\, d^3V < 0.1$ J, (3) ion heat loss due to convection $W_{convection} \approx 1.0 \pm 0.7$ J, and (4) estimated ion heat loss due to classical conduction $W_{conduction} \gtrsim 1.7 \pm 0.7$ J. (Ion energy loss to neutrals, predominantly via charge exchange, is estimated to be negligible.) The work done on the ions in V by compression is small, about 0.14 ± 0.28 J, and the classical viscous heating by ion flows is approximately 0.8 ± 0.5 J. This leaves approximately 2.3 ± 1.0 J, or $48 \pm 21\%$ of W_{rec}, which must have been converted to ion energy nonclassically. The remainder of W_{rec} goes to the electrons. W_{rec} is about 10 times larger than the expected energy release due to classical Ohmic dissipation, i.e., $E_\theta j_\theta \approx 10 \eta_{Sp} j_\theta^2$ (estimated $Z_{eff} \lesssim 1.2$). The energy balance confirms the necessity of nonclassical dissipation to explain the observed ion heating.

The relative importance of nonclassical versus classical dissipation is embodied in the ratio η^*/η_{Sp}, which was shown previously to scale inversely with collisionality [14]. By varying the discharge voltage, η^*/η_{Sp}, W_{rec}, and $\Delta W_{th,i}$ are varied. The correlation between $\Delta W_{th,i}$ and W_{rec} is quite strong as shown in Fig. 6(a), further supporting the claim that reconnection is indeed heating the ions. More suggestive, however, is the fact that the fraction $\Delta W_{th,i}/W_{rec}$ increases from approximately 4% to 14% as

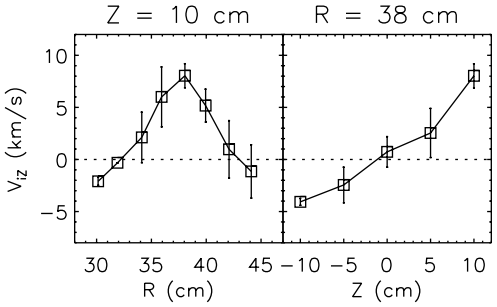

FIG. 5. Downstream ion drift speed V_{iZ} versus R at $Z =$ 10 cm (left) and versus Z at $R = 38$ cm (right) averaged over $t = 250$–270 μs (upstream $V_A \approx 35$ km/s).

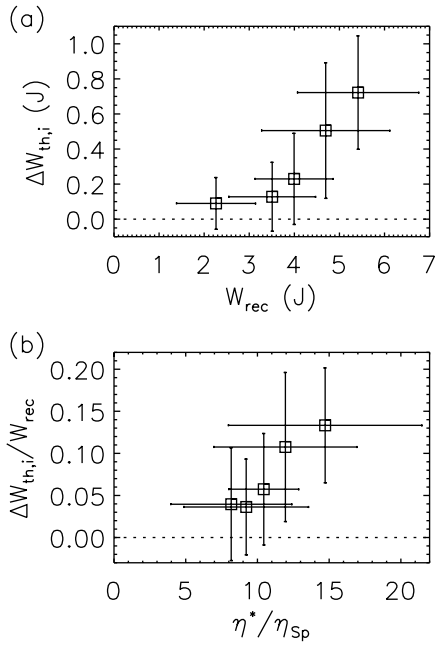

FIG. 6. Discharge voltage scan at constant helium fill pressure (6 mT). (a) Increase in ion thermal energy $\Delta W_{\mathrm{th,i}}$ versus reconnected magnetic field energy W_{rec} from $t = 245 \rightarrow 265$ μs in the reconnection layer. (b) Increase in $\Delta W_{\mathrm{th,i}}/W_{\mathrm{rec}}$ versus $\eta^*/\eta_{\mathrm{Sp}}$.

$\eta^*/\eta_{\mathrm{Sp}}$ increases from 8 to 15, as shown in Fig. 6(b). A possible explanation is that as the plasma becomes more collisionless, wave turbulence can scatter the current-carrying particles, increasing η^* and also heating the ions more effectively. However, other possible ion heating mechanisms which may arise in inertial reconnection models [11] cannot be ruled out at present. The subtle hint provided by Fig. 6(b) is that the same (nonclassical) mechanism which dissipates magnetic energy also heats the ions. This effect can provide a constraint on any mechanism proposed to explain the enhanced $\eta^*/\eta_{\mathrm{Sp}}$ observed in MRX.

To summarize, local ion heating due to reconnection has been demonstrated clearly using the novel IDSP diagnostic. This is a significant result because it has implications for many solar and space physics phenomena in which reconnection is invoked heuristically to explain the presence of energetic particles. It is estimated that more than half of the reconnected field energy is converted to ion thermal energy in MRX. The ion heating is attributed to nonclassical mechanisms because viscous heating by the observed sub-Alfvénic ion outflow and the energy available from classical Ohmic dissipation are both insufficient to account for the observed energy conversion to ions. The ion heating characteristics imply that nonclassical mechanisms such as wave-particle interactions and collisionless inertial effects could play an important role not only in determining the reconnection rate but also in heating the ions. It is worth noting that the "quiet-heating" scenario with no energetic flows observed in the present work could have implications for the problem of coronal heating. It is also worth noting that the absence of Alfvénic flows in MRX is understood to be a consequence of the high downstream pressure, suggesting that global boundary conditions should in general affect local reconnection dynamics. Theoretically, it is possible for current-driven instabilities to produce the observed effects presented in this paper, although collisionless inertial effects cannot be ruled out. Experimentally, efforts are underway to measure fluctuations in order to test the wave-particle hypothesis. A laser-induced fluorescence system under development will allow further studies of ion heating, including anisotropic effects, with much improved spatial and temporal resolution.

The authors thank D. Cylinder for technical assistance and Dr. F. Trintchouk, Dr. F. Levinton, and Dr. R. Bell for helpful discussions regarding the spectroscopy. S. C. H. and T. A. C. acknowledge support from NASA-GSRP. MRX is supported by NSF, NASA, and DOE.

*Now at Department of Applied Physics, California Institute of Technology, Pasadena, CA 91125.
†Permanent address: Department of Physics, University of Wisconsin–Madison, Madison, WI 53706.

[1] For example, V. M. Vasyliunas, Rev. Geophys. Space Phys. **13**, 303 (1975); D. Biskamp, Phys. Rep. **237**, 179 (1994).
[2] S. Masuda *et al.*, Nature (London) **371**, 495 (1994).
[3] E. R. Priest *et al.*, Nature (London) **393**, 545 (1998); see also E. N. Parker, *Spontaneous Current Sheets in Magnetic Fields* (Oxford University Press, New York, 1994).
[4] For example, J. W. Dungey, Phys. Rev. Lett. **6**, 47 (1961).
[5] For example, E. Scime *et al.*, Phys. Fluids B **4**, 4062 (1992).
[6] W. Gekelman, R. L. Stenzel, and N. Wild, J. Geophys. Res. **87**, 101 (1982).
[7] R. L. Stenzel, W. Gekelman, and N. Wild, J. Geophys. Res. **87**, 111 (1982).
[8] Y. Ono *et al.*, Phys. Rev. Lett. **76**, 3328 (1996).
[9] T. W. Kornack, P. K. Sollins, and M. R. Brown, Phys. Rev. E **58**, R36 (1998).
[10] For example, J. D. Huba, J. F. Drake, and N. T. Gladd, Phys. Fluids **23**, 552 (1980).
[11] For example, M. A. Shay, J. F. Drake, R. E. Denton, and D. Biskamp, J. Geophys. Res. **103**, 9165 (1998).
[12] M. Yamada *et al.*, Phys. Plasmas **4**, 1936 (1997).
[13] M. Yamada *et al.*, Phys. Rev. Lett. **78**, 3117 (1997).
[14] H. Ji, M. Yamada, S. Hsu, and R. Kulsrud, Phys. Rev. Lett. **80**, 3256 (1998); H. Ji *et al.*, Phys. Plasmas **6**, 1743 (1999).
[15] G. Fiksel, D. J. D. Hartog, and P. W. Fontana, Rev. Sci. Instrum. **69**, 2024 (1998).
[16] M. Hudis and L. M. Lidsky, J. Appl. Phys. **41**, 5011 (1970).
[17] For example, S. I. Braginskii, in *Reviews of Plasma Physics*, edited by M. A. Leontovich (Consultants Bureau, New York, 1965), Vol. 1, pp. 205–311.